Supporting Information

Sub-Nanometer Cu(I) Cluster: Coordination-modulated (Se *vs* S) Atom-Packing Mode and Emission

Feng Ke,[a,b] Yongbo Song,[a,b*] Hao Li,[a,b] Chuanjun Zhou,[a,b] Yuanxin Du,[a,b] and Manzhou Zhu[a,b*]

[a]Department of Chemistry and Centre for Atomic Engineering of Advanced Materials, Anhui Province Key Laboratory of Chemistry for Inorganic/Organic Hybrid Functionalized Materials, Anhui University, Hefei, Anhui 230601, People's Republic of China.
[b]Key Laboratory of Structure and Functional Regulation of Hybrid Materials, Anhui University, Ministry of Education, Anhui 230601, People's Republic of China.

Corresponding authors: ybsong860@ahu.edu.cn (Y.S.); zmz@ahu.edu.cn (M.Z.)

1. Experimental

1.1 Chemical

Copper(I) chloride (CuCl, ≥ 99.95%, metals basis), phenthiol (PhSH, ≥ 99.9%), phenylselenol (PhSeH, ≥ 99.9%), triphenylphosphine (PPh_3, ≥ 98%), sodium borohydride ($NaBH_4$, ≥ 99.99%), methylene chloride (CH_2Cl_2, HPLC, ≥ 99.9%), acetonitrile (CH_3CN, HPLC, ≥ 99.9%), methanol (CH_3OH, HPLC, ≥ 99.9%), ethanol (CH_3CH_2OH, HPLC, ≥ 99.9%). All reagents were used as received without further purification. All glassware was thoroughly cleaned with aqua regia (HCl : HNO_3 = 3 : 1 vol%), rinsed with copious pure water, and then dried in an oven prior to use.

1.2 Synthesis and crystallization of $Cu_{13}(SePh)_{13}(Ph_3P)_4$ clusters.

CuCl (40.0 mg, 0.40 mmol) was dissolved in 3 mL CH_3CN, and PhSeH (30 μL, 0.28 mmol) was dissolved in 15 mL methylene chloride. These two solutions were blended in a 100 mL flask. The solution was vigorously stirred with a magnetic stirring for 30 min. Then, Ph_3P (60 mg, 0.23 mmol. dissolved in 2 mL methylene chloride) were quickly added to the above solution. After ~30 min stirring, $NaBH_4$ (40 mg, 1.06 mmol, dissolved in 5 mL ice-cold nanopure water) were quickly added to the flask. The color of the solution changed from colorless transparency to black and finally to yellow transparent. The reaction was allowed to proceed 12 h at room temperature. After removing the aqueous phase, the mixture in the organic phase was dried and washed several times with CH_3OH to remove the redundant PhSeH and byproducts.

The $Cu_{13}(SePh)_{13}(Ph_3P)_4$ clusters were crystallized in CH_2Cl_2/CH_3OH for 3 – 4 days at room temperature. Yellow transparent crystals were collected, and the structure of Cu_{13} was determined by X-ray crystallography.

1.3 Synthesis and crystallization of $Cu_8(SPh)_8(Ph_3P)_4$ clusters.

The $Cu_8(SPh)_8(Ph_3P)_4$ cluster was synthesized with the similar synthetic method to that of Cu_{13} cluster, just changing the ligands from PhSeH to PhSH. The Cu_8 clusters were also crystallized in CH_2Cl_2/CH_3OH at room temperature. After 3 - 4 days, the green transparent crystals of Cu_8 were obtained.

1.4 The ligand-exchange of Cu_8 cluster with PhSeH.

10 mg $[Cu_8(SPh)_8(Ph_3P)_4]$ clusters were dissolved in 10 mL CH_2Cl_2. And then 10 μL PhSeH was added to the solution at room temperature. After ~8 hours, the mixture in the organic phase was dried, and then washed several times with CH_3OH to remove the redundant PhSeH and byproducts. The product was proved by fluorescence spectrometer, which shows same emission spectrum to that of Cu_{13} cluster (Fig. S4). Furthermore, the product was also crystallized in CH_2Cl_2/CH_3OH at room temperature, the crystal was determined by X-ray crystallography, which possesses same structure to that of Cu_{13} clusters (see detailed data in Section 2.1). These results demonstrate that the $[Cu_{13}(SePh)_{13}(Ph_3P)_4]$ also can be obtained by ligand-exchange from Cu_8 clusters.

2. Characterization

2.1 X-ray crystallographic determination of the Cu(I) clusters.

A suitable crystal was selected and performed on a 'Bruker APEX-II CCD' diffractometer. The crystal was kept at 296(2) K during data collection. Using Olex2[1], the structure was solved with the ShelXT[2] structure solution program using Intrinsic Phasing and refined with the ShelXL[3] refinement package using Least Squares minimisation.

1. Dolomanov, O.V., Bourhis, L.J., Gildea, R.J, Howard, J.A.K. & Puschmann, H. (2009), J. Appl. Cryst. 42, 339-341.
2. Sheldrick, G.M. (2015). Acta Cryst. A71, 3-8.
3. Sheldrick, G.M. (2015). Acta Cryst. C71, 3-8.

Crystal Data for Cu_{13} obtained by one-pot method: $C_{159}H_{143}Cl_{18}Cu_{13}P_4Se_{13}$ (M =4668.21 g/mol), triclinic, space group P-1, a = 17.6959(19) Å, b = 19.509(2) Å, c = 25.994(3) Å, α = 79.2200(10)°, β = 87.641(2)°, γ = 63.6130(10)°, V = 7888.1(15) Å^3, Z = 2, T = 296(2) K, μ(MoKα) = 5.110 mm^{-1}, *Dcalc* = 1.965 g/cm^3, 61767 reflections measured (2.598° ≤ 2Θ ≤ 54.28°), 31370 unique (R_{int} = 0.0523, R_{sigma} = 0.1056) which were used in all calculations. The final R_1 was 0.0620 (I > 2σ(I)) and wR_2 was 0.752 (all data).

Crystal Data for Cu_{13} obtained by ligand-exchange method: $C_{150}H_{125}Cu_{13}P_4Se_{13}$ (M = 3903.87 g/mol), triclinic, space group P-1, a = 17.726(5) Å, b = 19.518(5) Å, c = 26.004(7) Å, α = 79.241(3)°, β = 87.730(3)°, γ = 63.544(3)°, V = 7903(4) Å^3, Z = 2, T = 296(2) K, μ(MoKα) = 4.788 mm^{-1}, *Dcalc* = 1.641 g/cm^3, 61346 reflections measured (1.596° ≤ 2Θ ≤ 54.684°), 31403 unique (R_{int} = 0.0671, R_{sigma} = 0.1292) which were used in all calculations. The final R_1 was 0.0771 (I > 2σ(I)) and wR_2 was 0.2261 (all data).

Crystal Data for Cu_8 obtained by one-pot method: $C_{120}H_{100}Cu_8P_4S_8$ (M = 2430.67 g/mol), triclinic, space group P-1, a = 12.1898(12) Å, b = 14.6213(14) Å, c = 17.0179(16) Å, α = 73.7510(10)°, β = 70.7900(10)°, γ = 78.4410(10)°, V = 2730.1(5) Å^3, Z = 1, T = 296.15 K, μ(MoKα) = 1.787 mm^{-1}, *Dcalc* = 1.478 g/cm^3, 21401 reflections measured (2.604° ≤ 2Θ ≤

54.752°), 10887 unique (R_{int} = 0.0256, R_{sigma} = 0.0444) which were used in all calculations. The final R_1 was 0.0432 (I > 2σ(I)) and wR_2 was 0.1210 (all data).

2.2 Electrospray ionization mass spectrometry (ESI-MS) measurements is performed on MicroTOF-QIII high-resolution mass spectrometer. The samples are directly infused into the chamber at 5 μL/min.

2.3 X-ray photoelectron spectroscopy (XPS) measurements were performed on Thermo ESCALAB 250 equipped with a monochromated Al Kα (1486.8 eV) 150 W X-ray source, 0.5mm circular spot size, a flood gun to counter charging effects, and the analysis chamber base pressure lower than 1×10^{-9} mbar; data were collected with FAT = 20 eV.

2.4 Photoluminescence (PL) spectra were measured on a FL-4500 spectrofluorometer with the same optical density (OD) ~0.05. In these experiments, all fluorescence spectra were measured in the solid state of the clusters.

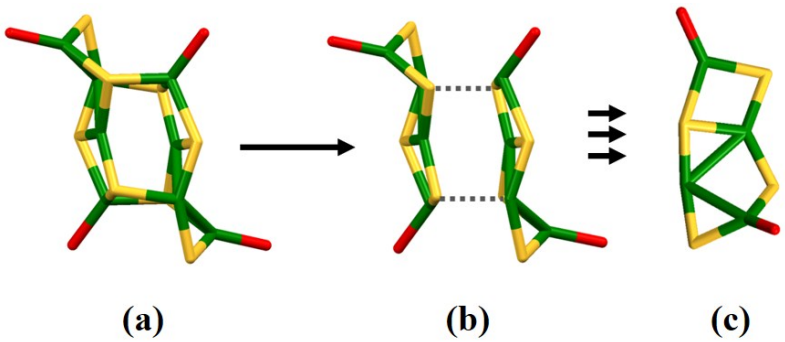

Fig. S1 Structural analysis of Cu_8 cluster: (a) and (b) top view; (c) side view of $Cu_4S_4P_2$ unit. Color labels: green = Cu; red = P; orange = S.

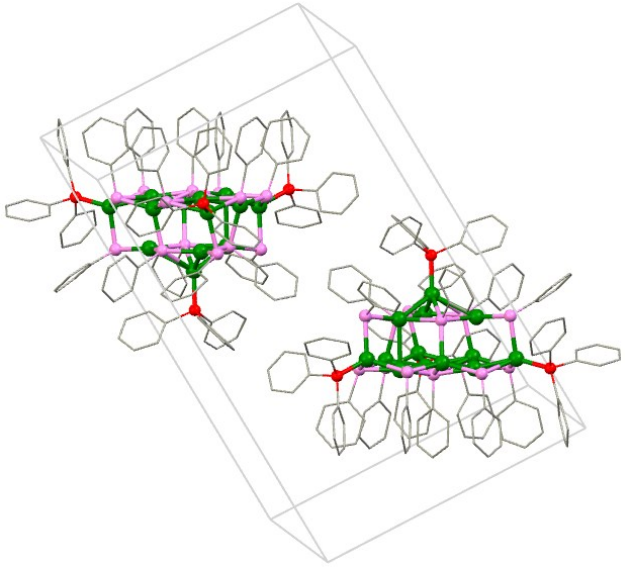

Fig. S2 Total structure of the Cu_{13} cluster. The unit cell contains a pair of left- and right-handed isomers. Color labels: green = Cu; red = P; violet = Se; gray = C.

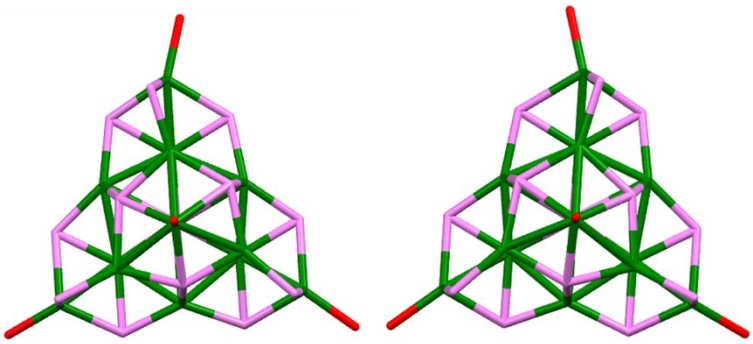

Fig. S3 Top views of two molecules of Cu_{13} in the same unit cell, which shows Cu_{13} is a chiral cluster. All of the C and H atoms are omitted for clarity.

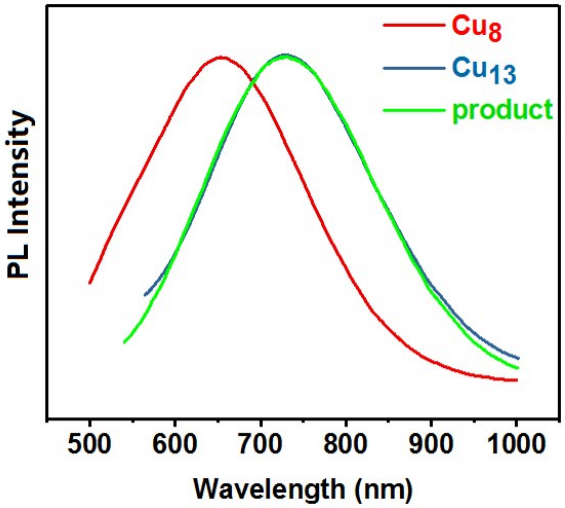

Fig. S4 Solid-state emission (λ_{ex} = 405 nm) spectra of Cu_8, Cu_{13} and the products obtained by ligand-exchange from Cu_8.

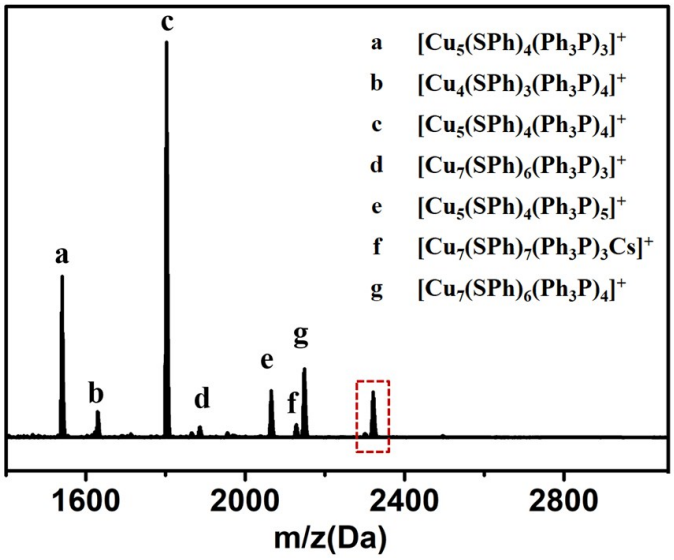

Fig. S5 ESI-MS spectrum of Cu_8 (in positive mode with adding Cs^+) and the assignment of the fragmentary peaks.

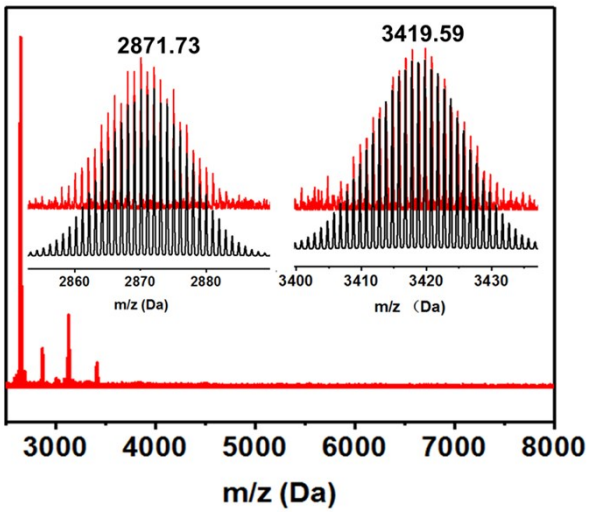

Fig. S6 The ESI mass spectra of Cu_{13} without adding Cs^+ in positive mode (inset: the comparison of the experimental and simulated isotope patterns).

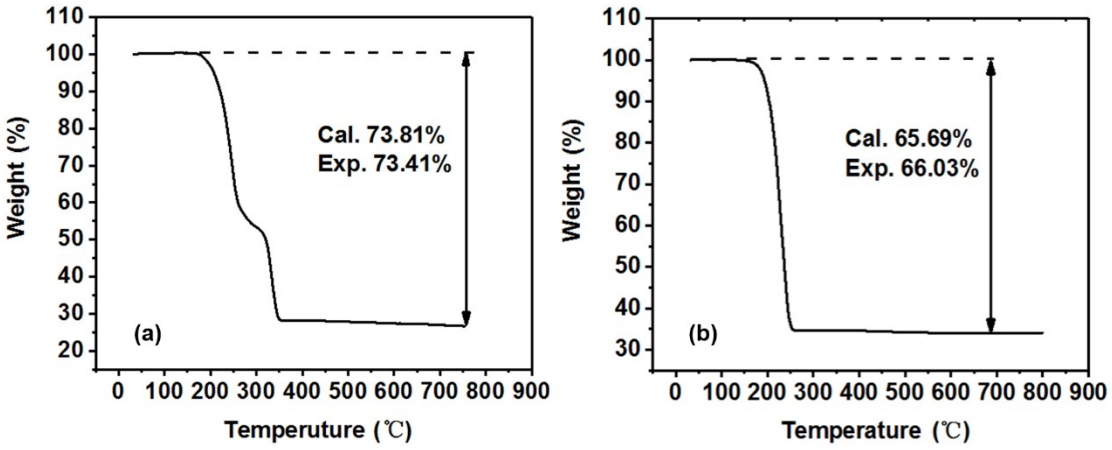

Fig. S7 TGA curves of Cu_8 (a) and Cu_{13} (b). Note: based on their weight loss, the product after calcination was assigned as Cu_2S and Cu_2Se, respectively.

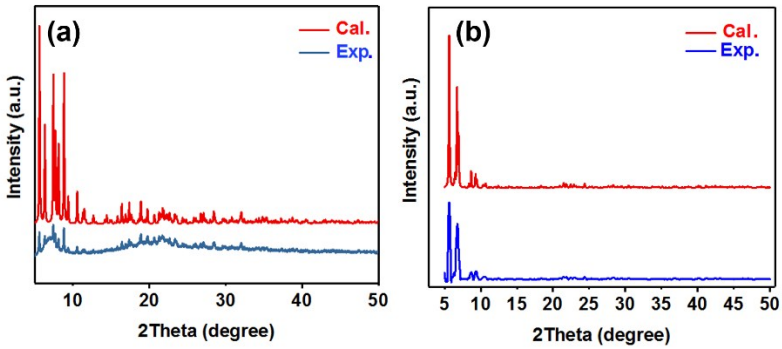

Fig. S8 Comparison of the experimental and theoretical powder X-ray diffraction curves of Cu_8 (a) and Cu_{13} (b).

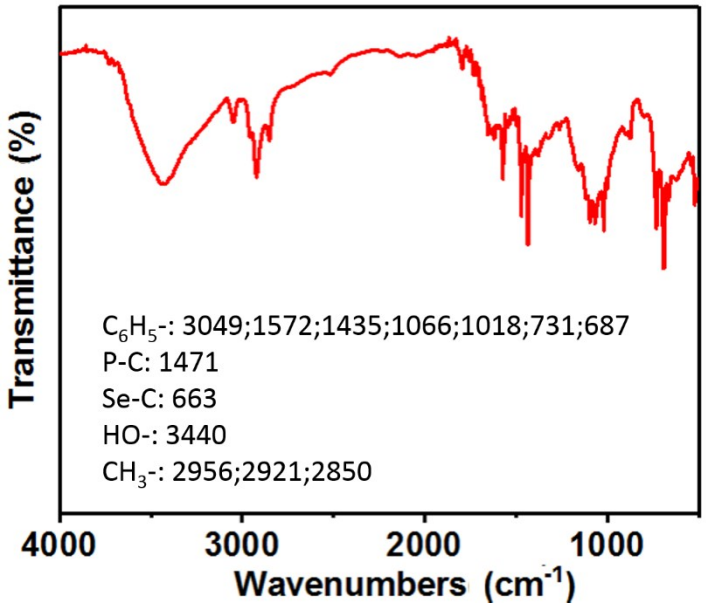

Fig. S9 The infrared spectroscopy of Cu_{13}, and the identification of correlation peaks.

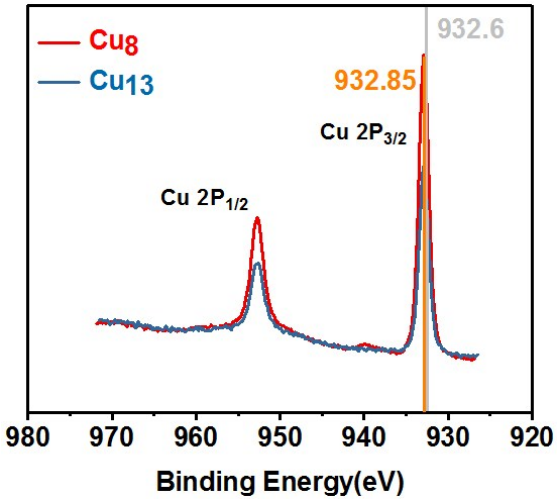

Fig. S10 XPS spectra of Cu_8 (red) and Cu_{13} (blue). Note: the binding energy of Cu(0) is 932.6 eV (gray line).

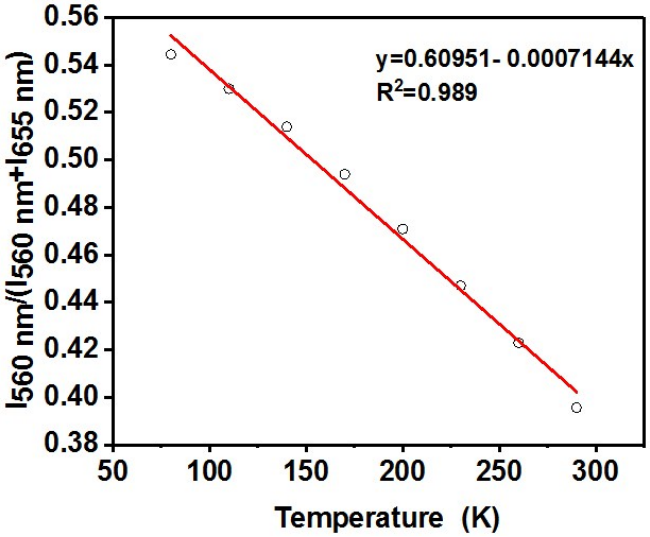

Fig. S11 The working curve and equation of the Cu_8 (λ_{ex} = 405 nm).

Table S1 Crystal Data and Structure Refinement for Cu_8 and Cu_{13}.

Compound	**Cu_{13}**	**Cu_8**
empirical formula	$C_{159}H_{143}Cl_{18}Cu_{13}P_4Se_{13}$	$C_{120}H_{100}Cu_8P_4S_8$
M_r	4668.21	2430.67
temperature/K	296(2)	296(2)
crystal system	triclinic	triclinic
space group	P-1	P-1
a/Å	17.6959(19)	12.1898(12)
b/Å	19.509(2)	14.6213(14)
c/Å	25.994(3)	17.0179(16)
α/°	79.2200(10)	73.7510(10)
β/°	87.641(2)	70.7900(10)
γ/°	63.6130(10)	78.4410(10)
volume/Å^3	7888.1(15)	2730.1(5)
Z	2	1
ρ_{calc} g/cm^3	1.965	2.276
μ /mm^{-1}	5.110	6.066
F(000)	4564.0	1783.0
reflections collected	61767	21401
R_{int}	0.0523	0.0256
data/restraints/parameters	31370/2106/1648	10887/720/631
goodness-of-fit	1.007	1.041
R_1/wR_2 [I 2σ(I)]^{a,b}	0.0620/0.1522	0.0432/0.1100
R_1/wR_2 [all data]^{a,b}	0.1187/0.1752	0.0635/0.1210
largest residuals e Å^{-3}	3.08/-1.04	1.59/-1.02